Available online at www.sciencedirect.com
SCIENCE DIRECT®
Continental Shelf Research 26 (2006) 943–958
CONTINENTAL SHELF RESEARCH
www.elsevier.com/locate/csr

Evaluation of the LISST-ST instrument for suspended particle size distribution and settling velocity measurements

Francisco Pedocchi*, Marcelo H. García

Ven Te Chow Hydrosystems Laboratory, Department of Civil and Environmental Engineering, University of Illinois at Urbana-Champaign, 205 North Mathews Ave., IL 61801, USA

Received 29 June 2005; received in revised form 17 March 2006; accepted 24 March 2006

Abstract

The Laser In Situ Scattering Transmissometry (LISST) instruments produced by Sequoia Scientific Inc. use light scattering to measure concentration and size distributions of sediment suspensions. In this article, the capabilities of the LISST-ST instrument are studied. The instrument reports the suspended sediment concentration and the settling velocity for eight different size classes by measuring the sediment concentration at the bottom of a small settling column. The size resolution of the LISST-100 and LISST-ST instruments is studied. This study utilizes a new inversion algorithm to obtain the size distribution from the scattered light pattern. In addition, attention is directed to observed deviations in laboratory measurements that may affect the relative concentrations and the settling velocity estimations. These deviations are analyzed in terms of: sample mixing problems; deviations on the settling of a suspension from its ideal behavior; and the effect of the shape of natural particles on laser scattering compared to that of spheres. Results suggests, of these three points the difference in the light scattering by irregular particles compared to the scattering by spheres is the main source of deviation on the settling velocity estimations. Finally, practical recommendations are given in order to gain confidence in the instrument results.

Keywords: Light scattering; Grain size; Particle concentration; Particle settling

1. Introduction

Measuring suspended sediment concentration is a difficult but important issue in sediment transport studies. Over the years, numerous techniques have been developed to measure sediment concentration using either acoustic or optical devices (Lynch et al., 1994; Fugate and Friedrichs, 2002; Wren et al., 2000; Creed et al., 2001). However, most of these techniques require instrument calibration for a specific particle size distribution, which poses a very important restriction in natural environments such as estuaries and continental shelves, where sediment size distribution is known to continuously change.

Even more difficult to achieve are in situ measurements of suspended sediment size distributions and particle settling velocities. These two quantities are especially relevant in fine sediment transport studies where the aggregation process controls the sediment deposition. For aggregates,

*Corresponding author. Tel.: +1 217 333 8365; fax: +1 217 333 0687.
E-mail address: pedocchi@uiuc.edu (F. Pedocchi).

0278-4343/$ - see front matter © 2006 Elsevier Ltd. All rights reserved.
doi:10.1016/j.csr.2006.03.006

the settling velocity cannot be inferred from the size of the particles, since particle density is not just a function of particle size (see Manning and Dyer, 1999). Therefore, in fine sediment research, independent measurements of the size and settling velocity of the particles are needed. Image analysis of video and photographic recordings has been used for this purpose (for example, Eisma et al., 1996; Mikkelsen et al., 2004, 2005). However, this technique presents limitations due to the large amounts of data involved, for both storing and processing the records. Also, wide size ranges are difficult to study, since high resolution is required to capture the smaller sizes but large pictures are needed to capture the larger and usually less abundant sizes.

In recent years, the application of the laser scattering technique has opened new possibilities for the in situ study of size distribution and particle settling velocities. Sequoia Scientific Inc. has developed a family of portable instruments, the Laser In Situ Scattering Transmissometry (LISST) series, which use the laser scattering technique for real time field measurements. These instruments appear to be more successful than other techniques used before and have become very popular. However, the laser scattering technique applied to the measurement of natural sediments suspensions presents specific difficulties that need to be taken into account to correctly analyze and interpret the data. Laboratory and field evaluations of the LISST series instruments have been published before by Agrawal and Pottsmith (2000), Traykovski et al. (1999) and Gartner et al. (2001). Among them, only Agrawal and Pottsmith (2000), the developers of the LISST instruments, have presented an evaluation of the settling velocity estimations made with the LISST-ST.

2. Size distribution of a settling suspension

In the LISST-ST, the suspension size distribution evolution is measured during a settling experiment, where particles settle in a 0.3 m high column placed over the laser beam. The settling velocity is computed from the concentration evolution of each size class at the bottom of the settling column.

To study the size distribution of a sediment suspension, the continuous size distribution is divided into a set of size classes. Each size class includes a narrow range of sizes, but not a unique particle size. In the case of the LISST instruments, these size classes are logarithmically spaced within the measurable particle size range. A size class j may be defined with a minimum and a maximum particle diameter $D_{\min,j}$ and $D_{\max,j}$, respectively. A mean diameter D_j of the size class can be associated with this range, and if the sizes are logarithmically spaced it may be defined as $D_j = \left(D_{\min,j}\, D_{\max,j}\right)^{1/2}$.

The minimum and maximum settling velocities for a particle size class j can be denoted as $w_{S\,j,\min}$ and $w_{S\,j,\max}$, respectively. For a settling column of length L and a given size class j, the time $T_{B\,j}$ that takes to the faster settling particles to disappear from the water column, and the time $T_{E\,j}$ that takes to the slower settling particles to disappear, are given as

$$T_{B\,j} = \frac{L}{w_{S\,j,\max}}, \tag{1}$$

$$T_{E\,j} = \frac{L}{w_{S\,j,\min}}, \tag{2}$$

respectively. If the particles are small enough and spherical, their settling velocities $w_{S\,j}$ can be computed using Stokes' law as follows:

$$w_{S\,j} = \frac{g}{18\nu}\left(\frac{\rho_{f\,j}}{\rho_w} - 1\right) D_j^2. \tag{3}$$

If a uniform density within each size class is considered, $T_{B\,j}$ and $T_{E\,j}$ will only be functions of the density of the particles of each size class ($\rho_{f\,j}$) and the water properties, kinematic viscosity (ν) and density (ρ_w). Therefore, using Eq. (3) $T_{B\,j}$ and $T_{E\,j}$ will be related according to the equation

$$\frac{T_{E\,j}}{T_{B\,j}} = \left(\frac{D_{\max,j}}{D_{\min,j}}\right)^2. \tag{4}$$

The concentration of each size class $V_{T\,j}(t)$, with initial size distribution $V_j(0)$, at the bottom of the settling column can be computed using Stokes' settling law,

$$V_{T\,j}(t) = \begin{cases} V_j(0) & \text{for } 0 < t < T_{B\,j}, \\ V_j(0)\left[1 - \dfrac{t - T_{B\,j}}{T_{E\,j} - T_{B\,j}}\right] & \text{for } T_{B\,j} < t < T_{E\,j}, \\ 0 & \text{for } T_{E\,j} < t. \end{cases} \tag{5}$$

Using these definitions, a simulated concentration history can be obtained, as shown in Fig. 1. This simulated concentration history is for spherical

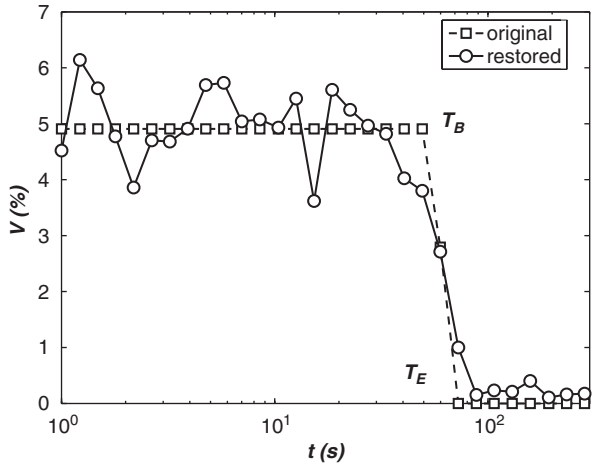

Fig. 1. Original and restored theoretical concentration history of one of the 32 sizes classes using the IPA algorithm (see Section 4.1). The theoretical suspension is composed of spherical particles with diameters between 66.48 and 78.45 μm, and density equal to 2650 kg/m^3. The sloped part starts at time T_B and ends at T_E corresponding to the times that take to the larger and smaller particle within the size class to travel from the top to the bottom of the settling column ($L = 30$ cm) in still water at 20 °C. Noise of 1% amplitude was added to the computed power signal before restoring the size distributions. The threshold used to stop the iteration was 10^{-6} and the parameter α used was equal to 0.2.

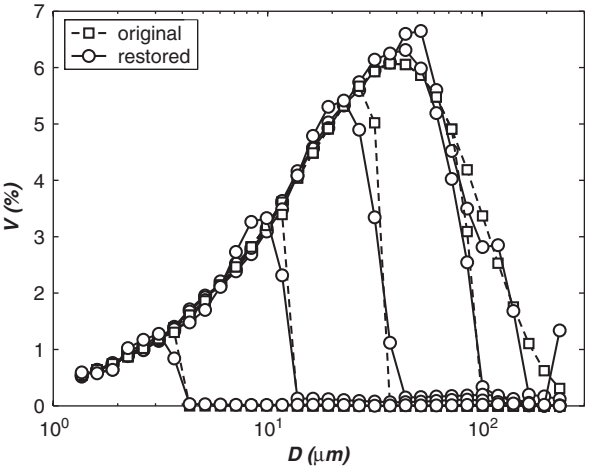

Fig. 2. Original and restored (using the IPA algorithm, see Section 4.1) size distribution evolution for a theoretical settling experiment of an arbitrary initial suspension of spherical particles of density 2650 kg/m^3 at the bottom of a settling column in still water at 20 °C. The symbols correspond to the volume concentration value on each of the 32 log-spaced size classes as a percentage of the total initial concentration. The measurement times are 1, 40.5, 284, 2000 and 20,300 s. Noise of 1% amplitude was added to the computed power signal before restoring the size distributions. The threshold used to stop the iteration was 10^{-6} and the parameter α used was equal to 0.2.

particles with density equal to 2650 kg/m^3 (quartz) in water at 20 °C, and for a size class that includes particles with sizes between 66.48 and 78.45 μm. For the same conditions, the evolution of the size distribution computed for an arbitrary settling suspension at the bottom of the settling column is shown in Fig. 2 for times t =0, 40.5, 284, 2000 and 20,300 s.

In the above deduction of the settling velocity, each particle was assumed to behave as it was settling alone in still fluid. However, it has been shown that this assumption is not exactly correct for a particulate suspension even with very small concentrations. Batchelor (1972) studied the sedimentation of a dilute dispersion of uniformly sized spheres and showed that the mean settling velocity of the spheres can be approximated to the first order as

$$w_S = w_{S0}(1 - 6.55\ V), \tag{6}$$

where w_S is the mean value of the settling velocity of spheres inside de suspension, w_{S0} is the settling velocity a single sphere in clear fluid and V is the volume concentration of the suspension.

The study of the fluctuations around this mean settling velocity value is source of current research that show that the sedimentation of a dilute suspension of spheres is much more complex than expected: refer to the experiments by Segre et al. (1997) and Bergougnoux et al. (2003). These researchers report large fluctuations in the settling velocity of the particles, on the order of the mean setting velocity, and higher spreading of the settling front that the ones predicted by Eq. (4).

3. Description of the device

3.1. Laser scattering for particle sizing

The physical basis of light scattering theory for particles very large compared to the light wavelength is briefly explained in this section. When light rays reach a particle 20 or more times larger than the light wavelength, it is possible to separate these rays into two groups, those hitting the particle surface and those passing along the particle (van de Hulst, 1981). The rays that do not enter into the particle are diffracted around the particle at small angles around the forward direction with a certain pattern that is related to its shape and size but not to its surface characteristics (van de Hulst, 1981; Agrawal and Pottsmith, 1994). The rays that enter

the particle are refracted, reflected and absorbed in all spatial directions depending on the particle shape and composition. While the intensity in the forward direction due to this latter phenomenon is smaller than that due to diffraction, dependence in the measurements on particle composition should be expected.

In practice, the scattered light is measured by a discrete number (N) of photosensitive detectors placed at different angles, each of them covering an angle range. If the particles are sparsely distributed, the relation between the scattered light power and the different particle size classes is given by a linear relation. Using index notation, such relation can be expressed as

$$E_i = K_{ij} V_j, \tag{7}$$

where E_i is the light power distribution over the N detectors ($i = 1, 2, \ldots, N$), V_j is the volume distribution expressed in N sizes classes ($j = 1, 2, \ldots, N$), which can be estimated with

$$V_j \propto \int_{D_{j,\,\min}}^{D_{j,\,\max}} D^3 n(D)\,\mathrm{d}D, \tag{8}$$

and $D_{j,\,\min}$ and $D_{j,\,\max}$ are minimum and maximum particles diameters in the jth class and $n(D)$ is the number of particles of size D. The kernel matrix K_{ij} is used to compute the light that is scattered by the jth class of particles into the ith detector.

3.2. Implementation of the laser scattering for particle sizing into the LISST instruments

The LISST-100 and LISST-ST instruments measure the scattered light with 32 logarithmically spaced, ring-shaped detectors. The kernel matrix is provided by Sequoia Scientific Inc., developers of LISST. The kernel matrix was computed for spheres using the full Lorenz–Mie theory model for scattering, which allows taking into account the effect of the refractive index and the measurement of the scattered energy at large angles. Therefore it gives a better description of the laser scattering pattern than the one obtained by Fraunhofer diffraction theory (de Boer et al., 1987; Agrawal and Pottsmith, 1994; Wedd, 2003).

The kernel matrix relates the scattered light distribution with the area distributions (cross-section) of the particles but can be adapted to relate the volume-distribution of the particles. Assuming that particles are spherical,the area distribution has to be multiplied by the diameter of the particle size class associated with it to get the volume distribution.

The scattered power that is measured during an experiment $\widehat{E}_i$ must be corrected to take into account the background scattering z and the optical transmission τ. In the center of the light detectors, a photo-diode measures the light that was not absorbed or scattered by the particles and records the values of the optical transmission τ. Before starting a series of experiments, the background scattering distribution z should be measured using clear water to take into account imperfections that could exist in the device optics and the scattering and attenuation due to the water itself. If $\widetilde{E}_i$ is the corrected scattering distribution, this can be expressed as

$$\widetilde{E}_i = \left(\widehat{E}_i \Big/ \tau\right) - z. \tag{9}$$

Finally, the power distribution needs to be corrected for the non-ideal detector responsivity. Using a correction factor for each ring ${}_i\kappa$, which are provided by the instrument maker, the fully corrected scattered power distribution E_i is obtained as

$$E_i = {}_i\kappa \widetilde{E}_i \tag{10}$$

Here the index before the symbol (${}_i\kappa$) is used to indicate that the correction factor is different for each detector, but in this case the sum over the repeated index should not be performed, as it regularly must be done when using index notation.

Once the power distribution E_i is known, the volume distribution V_j can be obtained by solving Eq. (7), which is a mathematically ill-posed system (the solution to Eq. (7) is discussed in Section 4.1). The distribution has to be corrected by a volume conversion factor C_V. This conversion factor takes into account the electronic characteristics of the device and should be determined empirically by testing the device with known particle size distributions (Agrawal and Pottsmith, 2000). The full corrected size distribution is finally obtained as

$$V_j = \frac{1}{C_V}\left(K_{ij}^{-1} E_i\right). \tag{11}$$

The main advantage of the LISST instruments compared to other optical techniques, such as light backscatter or light transmission, is that the conversion factor C_V can be considered a constant

for all size distributions, while with these other instruments variations of one or two orders of magnitude may be expected depending on the particle size distribution (Baker and Lavelle, 1984; Wren et al., 2000). Nevertheless, variations up to 300% in C_V with the mean size of monosize distribution, were reported by Gartner et al. (2001). For the device studied, the same tendencies were found but a careful analysis showed that a large part of the deviation could be attributed to insufficient mixing of the samples, at least for the experiments reported here. Detailed explanation and discussion of this phenomenon are presented in Section 5.1.

3.3. The LISST-ST

As explained in Section 3.2 the LISST-ST measures the sediment concentration and size distribution in the same way as the LISST-100 instrument. The difference is that the LISST-ST has a 0.3 m settling column over the laser beam path, and instead of measuring the environment sediment concentration and size distribution, it measures the size distribution during the settling experiment. This is done by introducing a water sample into the settling column and measuring its size distribution at prefixed times. This allows the study of concentration changes over time at the bottom of the settling tube for the different size classes.

The software provided with the LISST-ST by Sequoia Scientific Inc. adds the 32 signals of the power distribution in groups of 4 to obtain an 8-class power distribution. For this 8-class power distribution the 8×8 kernel matrix for size-area distribution is provided by Sequoia Scientific Inc. According to Sequoia Scientific Inc., adding the scattered light signal in group of 4 reduces the noise in the signal, assuring statistical independence of the inversion results and avoiding the inter-contamination between adjacent size classes (Sequoia Scientific Inc., 2005). Another option is to restore the 32 size volume distribution using the 32×32 kernel matrix that is used with the LISST-100 instruments and then add the 32 size classes in groups of 4 to finally get 8 broader size classes. Both procedures were observed to produce essentially the same results.

Assuming that the particles have uniform density inside each size class, the LISST-ST software adjusts a model of concentration history of the form of Eq. (5) to the measured history. This is accomplished via a least-squares approximation with T_{Bj} as a parameter which is selected in order to get the best fit between the measured history and the model. The model for the concentration history $V_{Cj}(t)$ is defined as (Agrawal and Pottsmith, 2000)

$$V_{Cj}(t) = \begin{cases} \frac{1}{T_{Bj}} \int_0^{T_{Bj}} V_j(t)\,\mathrm{d}t & \text{for } 0 < t < T_{Bj}, \\ V_j(T_{Bj}) \left[1 - \dfrac{t - T_{Bj}}{T_{Ej} - T_{Bj}}\right] & \text{for } T_{Bj} < t < T_{Ej}, \\ 0 & \text{for } T_{Ej} < t. \end{cases} \tag{12}$$

where T_{Bj} and T_{Ej} are defined as in Eqs. (1) and (2), and are related according to Eq. (4).

The ratio between the maximum and minimum particle diameter inside a size class presented in Eq. (4) is a constant for all size classes in the log-spaced size distributions measured by the LISST instruments. Therefore, if Stokes' law applies and particles have uniform density, T_{Bj} is the only parameter selected in the fitting process. For a log-spaced size distribution, $T_{E,j}/T_{B,j} = \left(D_{\max,j}/D_{\min,j}\right)^2 = (S^{1/N})^2$, where $S = D_{\max}/D_{\min}$ is the dynamic range of the detectors, $D_{\max}$ and $D_{\min}$ are the maximum and minimum particle diameter that the instrument measures, and N is the number of size classes in the measured range. S is equal to 200 in the newer LISST-100 and LISST-ST instruments and 100 in the older ones; N is equal to 32 in the LISST-100 and equal to 8 in the LISST-ST. $D_{\max}$ and $D_{\min}$ are equal to 250 and 1.25 μm in the Type B instruments and 500 and 2.25 μm in the Type C instruments.

With this fitting the possible deviations due to noise in the signal are expected to be filtered out. The initial concentration for each size class is assumed equal to the first line in Eq. (12) and the average settling velocity for each size class w_{Sj} is computed from the selected T_{Bj} using

$$w_{Sj} = \frac{L}{T_{Bj}\, S^{1/N}}. \tag{13}$$

However, if the difference between the fitted model and the measured concentration history is large, the fitting could lead to wrong initial concentration and settling velocity estimations. This is one of the main problems that the LISST-ST presents and it will be discussed in detail in Section 5.3.

4. Laser scattering particle sizing problems

4.1. The data inversion problem

Solving Eq. (7) gives the size distribution from the measured light power distribution. The kernel matrix K_{ij} is mathematically ill-posed so even the presence of low noise levels in the scattered light signal may produce unexpected solutions. Therefore, regular inversion cannot be used to solve the system. Riley and Agrawal (1991) studied different inversion algorithms. The standard software that comes with the LISST instruments uses one of these algorithms (called here NLIA). The algorithm is a modified version of the Chahine inversion method (Chahine, 1970); older versions of the software used the Phillips-Towomey algorithm (Twomey, 1977).

We developed and tested our own inversion algorithm (IPA), an improved version of the projection algorithm presented by Huang et al. (1975) and modified by Jianping et al. (2001). Its capabilities were studied carefully (see Pedocchi and García, 2006) and only a brief description of the algorithm is presented here. The projection algorithm starts from an initial guess solution $V_j^{0,1}$, which is subsequently improved. A general step in the iterative process can be described as

$$V_j^{I,n} = V_j^{(I-1),n} - \frac{1}{n^{\alpha}} \left(\frac{K_{Ij}\, V_j^{(I-1),n} - E_I}{K_{Ij}\, K_{Ij}} \right) K_{Ij}, \qquad (14)$$

In Eq. (14), n is the iteration cycle, I is the step into the cycle and α is a parameter between 0 and 1 that allows to set the noise resolution trade-off. The number of I steps in each cycle is given by the number of size classes N. For example, N is equal to 32 in the LISST-100.

By measuring the convergence of the algorithm, a criterion to stop the iterative process is defined. The residual after each iteration cycle is defined as

$$R^{I,N} = \frac{\left(E_i - K_{ij} V_j^{I,N}\right)^2}{(E_i)^2} \quad \text{for } E_i \neq 0. \qquad (15)$$

The iteration is stopped when two consecutive residuals differ by less than a threshold value.

The parameter α should be chosen according to the levels of noise and the shape of the size distribution. Spread size distributions and high levels of noise require values of α near one. Narrow distributions and low noise levels allow the use of values of α near zero. The highest resolutions are achieved for smaller values of α. For the noise levels present in the LISST instruments, α equal to 0.2 gives accurate results and no deviations can be attributed to the inversion process (Figs. 1 and 2).

Restoring the size distribution of a settling suspension presents some particular characteristics that must be taken into account. In each sample time, the size distribution of the particles that remained in suspension is restored (Fig. 2). It is very important to solve the sharp side of the distribution correctly, otherwise the algorithm will wrongly show particles classes where no particles remain in suspension. Computer-simulated distributions and the corresponding restored distributions using the improved projection algorithm for 32 size classes are shown in Fig. 2. One of the 32 size class concentration histories is shown in Fig. 1. No important differences are found between the original and the restored one. Before starting the restoring process, a 1% amplitude noise, which is much higher than the noise level expected in the LISST signal under normal operation conditions, was added to the computed power signal.

Finally, comparison between the new IPA algorithm and the NLIA algorithm provided with the LISST instruments is performed here. Figs. 3 and 4 show the results for both algorithms for a sharp monosize distribution and a bimodal distribution of ground silica particles. The IPA algorithm clearly

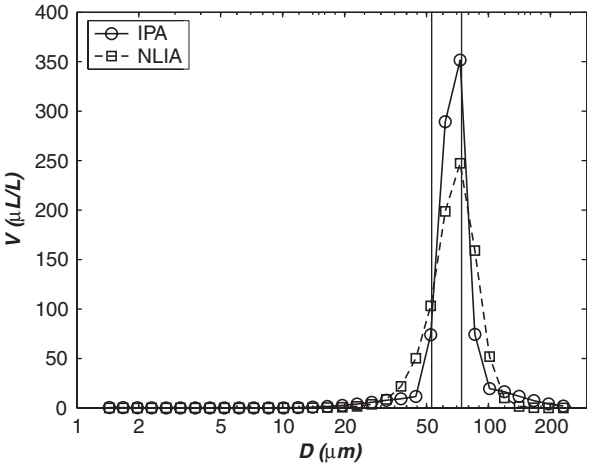

Fig. 3. Comparison of the restored size distributions obtained using the IPA and NLIA inversion algorithms. The sharp peak of the monosize distribution of particles between the 53 and 74 μm sieves (indicated with vertical lines) is better captured by the IPA algorithm. The threshold used to stop the iteration was 10^{-6} and the parameter α used was equal to 0.2.

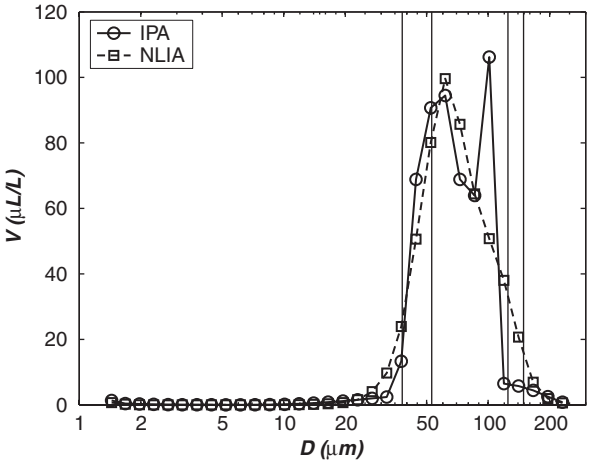

Fig. 4. Comparison of the restored size distributions obtained using the IPA and NLIA inversion algorithms. The two peaks of the bimodal size distribution are only captured by the IPA algorithm. The two monosize distributions used to prepare the mixture were retained between the 38 and 53 μm, and the 125 and 149 μm sieves. The threshold used to stop the iteration was 10^{-6} and the parameter α used was equal to 0.2.

presents higher resolution that NLIA algorithm without noise amplification.

4.2. Effect of the shape of the particles

A more complicated source of deviations in the size distribution measurements is the effect of the shape of the particles. The kernel matrix that is used for processing the light power signals recorded by the LISST instruments was developed for spherical particles. However, a non-spherical particle is known to create a diffraction pattern different from that of spherical one of equivalent size (see for example, Fischbach et al., 1985) which may affect the accuracy of the particle size measurement.

Jones (1987) and later Al-Chalabi and Jones (1993) mathematically modeled the Fraunhofer diffraction patterns of random irregular particles. Their computations suggested that over a limited range of irregularity sizes and for angles close to the forward direction, the irregular particles produced a diffraction pattern that might be modeled as a set of spheres with a size distribution given by the distribution of the irregularities. The inversion of this scattered light pattern will artificially produce a broader size distribution reducing the resolution that can be achieved from inverting the diffracted light pattern.

Mühlenweg and Hirleman (1998) reported that although the particle microstructure (i.e. its surface roughness) has no effect on the light scattering, the particle macrostructure (i.e. its axis ratio) has an important influence on the light scattering. They suggested corrections to the standard theory for spheres, but the axis ratios of the particles should be known in advance by a three-dimensional shape analysis. Therefore, calibration for each type of particle is needed.

Matsuyama et al. (2000) discussed the diffraction due to randomly orientated ellipsoids. They concluded that if the particle size distribution is wide enough with respect to the aspect ratio of the ellipsoids, and they are randomly oriented, a peak appears at the size of the minor axis. Otherwise two peaks should appear, corresponding to the minor and major diameters of the ellipsoid.

Direct measurements of light scattering by different types of randomly oriented natural particles have been performed in the last years in Amsterdam, mainly for astronomic applications (Hovenier, 2000). Results have been reported for a number of hydrosols (Volten et al., 1998) and aerosols (Volten et al., 2001; Muñoz et al., 2001; Hovenier et al., 2003). Liu et al. (2003) compared these results with the ones given by Lorents–Mie theory for spheres, concluding that this theory does not hold for most scattering angles. These studies motivated by their astronomical application covered a very wide range of angles over all the spatial directions. Due to experimental limitations, the measured angle range was initially 5° to 173°, which was recently expanded to 3° to 174° (Hovenier et al., 2003). Therefore, no experimental results are available for the small forward angles which are the ones of more interest for our application. However, the deviations observed for the smaller angles are not particularly large and the researchers used the Lorenz–Mie theory to complete the measurements in the forward region (Hovenier et al., 2003; Liu et al., 2003).

Another type of irregular particulate systems is those of aggregates. Aggregate systems may be divided into aggregates of small particles, of the order of the wavelength and aggregates of large particles, as defined in Section 3.1 (Stone et al., 2002). In the latter, which are the most relevant for the applications involved in sediment transport, the overlapping effects of the aggregate constitutive particles become significant (Stone et al., 2002; Mühlenweg and Hirleman, 1999). Therefore, for compact aggregates one would expect each aggregate to behave as an irregular particle, as the solid

particles described above. However, for macro aggregates formed by many smaller and more compact aggregates, the light would be scattered by this smaller compact units (Gustafson, 1999), making difficult to capture the actual size of the larger structure that they form.

Based on the information available it is clear that extremely large deviations from the spherical particles theory should not be expected in the sizes estimated using forward light scattering with irregular particles. However, the exact shape of the size distribution and the resolution that could be achieved will be degraded. This would also affect the settling velocity estimations as will be explained in Section 5.5. Until a way to correct the size distribution deviations produced by shape effects is available, users should be careful with the conclusions they draw out of their measurements, specially concerning details of the size distribution.

5. Laboratory experiments and discussion

Results from a group of experiments done with ground silica are presented here. Sieves were used to separate particles of different sizes. The ground silica is a cohesionless sediment and the suspension was prepared from dried sediment samples just before the experiments, therefore no cohesion effects due to biological activity should be expected. The samples were then energetically mixed in a container prior to pouring the suspension inside the settling column. The measurements started approximately one second after the sample was poured. Special care was taken to keep all the particles in suspension while pouring the sample. Care was also taken to avoid excessive number of bubbles in the settling column. The IPA algorithm was used to invert the 32 size class scattered light signal.

5.1. Concentration estimation variations

The variation of the measured volume concentration over the mass concentration as a function of the measured mean diameter of mono- and bimodal size distributions is showed in Fig. 5. Since the silica particles have uniform density, the measured volume concentration over the mass concentration is proportional to the volume conversion factor C_V. The variation of C_V with the mean size for monosize distributions may affect the shape of well-sorted size distributions since it tends to underestimate the concentration at the larger size classes.

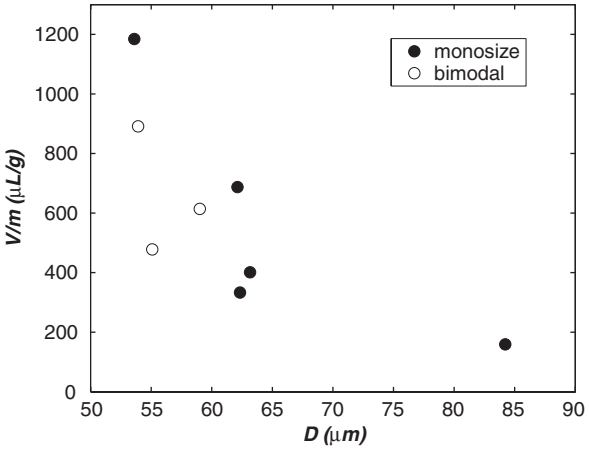

Fig. 5. Volume over mass, which is proportional to the volume conversion factor C_V, computed using the IPA algorithm as function of the measured mean particle diameter, for both monosize and bimodal distributions. Clearly C_V increases as the particle size decreases.

The results presented in Fig. 5 are in agreement with those of Gartner et al. (2001), who reported variations up to a factor 3 in C_V with the mean size of a wide range of monosize distributions. On the other hand, Agrawal and Pottsmith (2000) report no dependence of C_V on the particle size as well as Traykovski et al. (1999). However, these last researchers only reported C_V results for two neighboring sizes ranges 5–25 and 25–63 μm. Y. C. Agrawal (personal communication) suggested that the variation in the volume concentration estimates might be due to insufficient mixing of the samples, and proposed to study the relation between the light transmission and the area concentration, both measured and reported by the LISST. The logarithm of the inverse of the light transmission is proportional to the cross-section area concentration of the suspension, with only a weak dependence on the particle characteristics (McCave and Gross, 1991; Clifford et al., 1995). The results are plotted in Fig. 6 which shows a well defined proportionality between the transmission and the projected area of the samples computed from the light scattering.

The remaining turbulence in the column after pouring the sample could be responsible of keeping small particles in suspension, while the larger, less numerous particles might start to settle. This could eventually generate a non-uniform initial concentration profile within the settling column. However, in experiments with sediments with broad size distributions, both the concentration computed from the scattered signal and the transmission

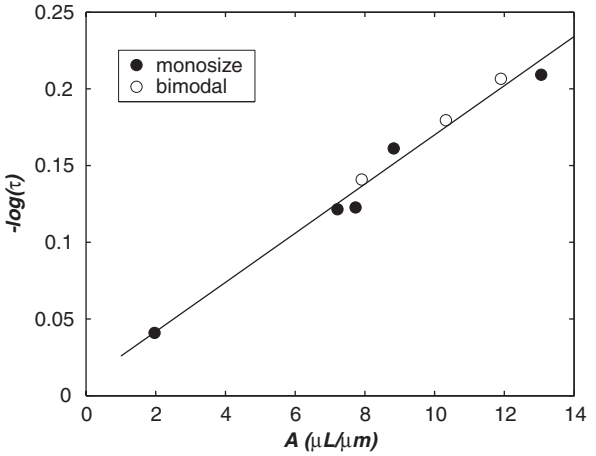

Fig. 6. Relation between the cross-section area concentrations measured from the inversion of the scattered light and the logarithm of the inverse of the transmission for the experiments plotted in Fig. 5. The very clear correlation between these two quantities suggests that mixing problems caused the variation of C_V observed in Fig. 5.

remained constant for approximately the first 10 s, suggesting that these effects cannot be very important Fig. 11.

Traykovski et al. (1999) also used a LISST-ST in their evaluation of the LISST instruments. However, they did not report any important variation in the concentration estimations with the particle size, probably because of the small and very similar sizes they used. The transmission values they reported seem to verify the proportionality with the area concentration. They did not clearly explain the experimental procedure followed to place the suspension in the LISST-ST sampling volume. Gartner et al. (2001) used a mixing device to keep all the particles in suspension inside a measuring chamber attached to a regular LISST-100 instrument. They reported that the concentration estimated by the LISST tend to increase as the particle size decreased, but unfortunately they did not report the transmission values for their experiments making impossible to know if mixing problems caused their concentration estimation variations.

5.2. Size distribution resolution

In this section, bimodal size distributions are studied. A bimodal suspension was prepared by mixing particles of two different sizes. Fig. 7b shows the raw results for a mixture of particles with sizes 38–53 and 125–149 μm, the light scattered signals

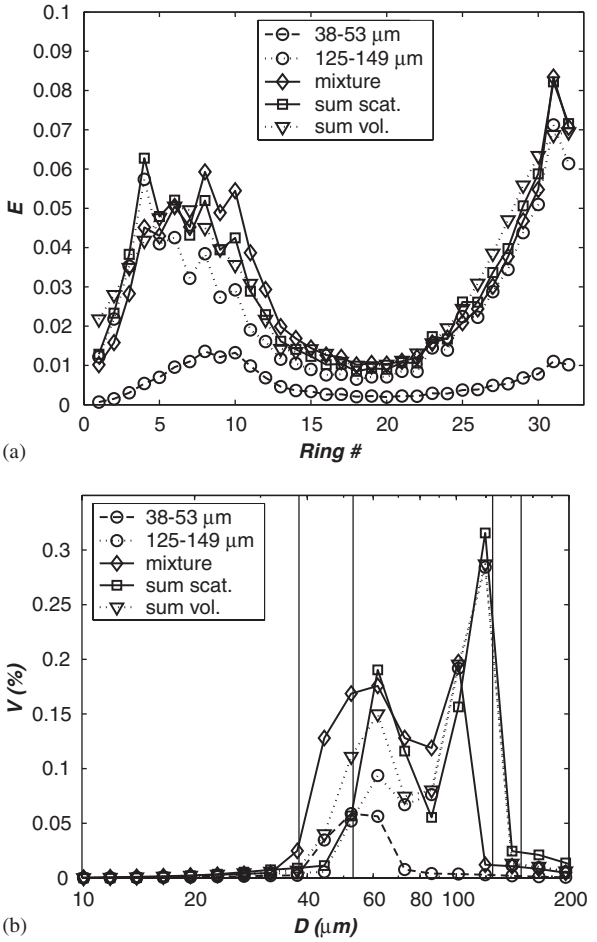

Fig. 7. Scattered light pattern (a) and inverted size distribution (b) for a bimodal suspension [18% (38–53 μm) + 82% (125–149 μm)]. The percentages correspond to the relative masses that were used to prepare the suspension, as described in Section 5.2. "mixture" corresponds to the actual measurement of the particles mixture (Point 2, in Section 5.2); "sum scat." corresponds to the sum of the power signals in the above proportion (Point 3); "sum vol." corresponds to the sum of the volume distributions of the individual monosize distributions in the above proportion (Point 4).

are also shown in Fig. 7a. The procedure followed to produce these plots was as follows:

(1) Two monosize distributions composed of particles that were captured between two consecutive sieves were measured. The sieves apertures are indicated with vertical lines in the figures. Note that the peaks are not exactly inside the ranges in every case; this may be due to the effect of the shape of the particles. Note also that the accuracy of the sieves, under 74 μm is limited and for these reason they are not included in the

standard soil characterization tests (ASTM D422-63, 2002).

(2) A mixture of particles of two different sizes was also measured and the power signal inverted in the same way as for the monosize distributions.
(3) The power signals of each monosize distribution of Point (1) were added, using the mass proportion that was used for the mixture in Point (2). This power signal was inverted and a size distribution was obtained.
(4) The two monosize distributions of Point (1) were added and the power distribution of the mixture was obtained using Eq. (7) to allow the comparison with the distributions of Points (2) and (3).

From Fig. 7 it is clear that although the two peaks are captured, the relative amount of particles in each size is not correctly restored. Observing the scattered light distribution, it is clear that the power distribution of the mixture is very different from both the addition of the individual size power signals (Point 3) and particle size distributions (Point 4). However, if it is assumed that the problem is due to insufficient mixing and that the actual proportion between sizes in the sampling volume was different from the initially measured mass proportion, one may try to adjust the proportion between the sizes used in Points (3) and (4) in order to obtain a power signal as close as possible to the measured one. The result for this best proportion is shown in Fig. 8 where all the three bimodal size

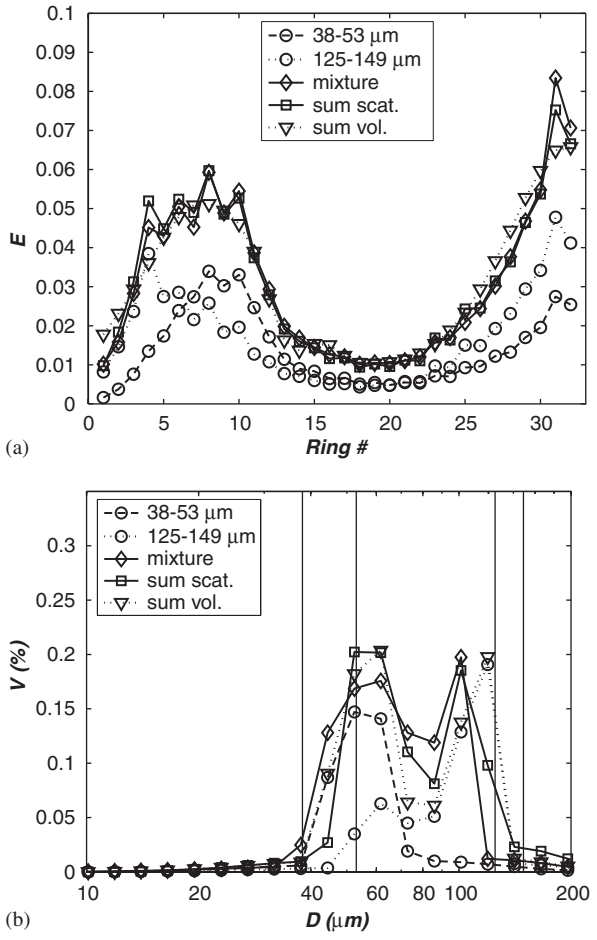

Fig. 8. Scattered light pattern (a) and inverted size distribution (b) for a bimodal suspension assumed to be composed by [45% (38–53 μm) + 55% (125–149 μm)]. The percentages correspond to the relative concentration that gives the best combined scattering distribution, as described in Section 5.2.

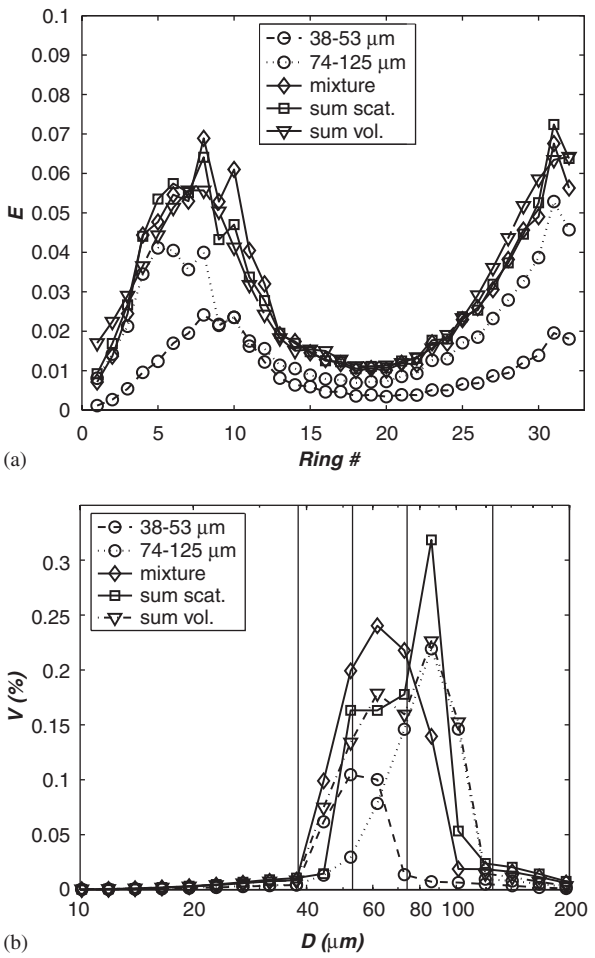

Fig. 9. Scattered light pattern (a) and inverted size distribution (b) for a bimodal suspension [32% (38–53 μm) + 68% (74–125 μm)] according to the relative masses that were used to prepare it, as described in Section 5.2.

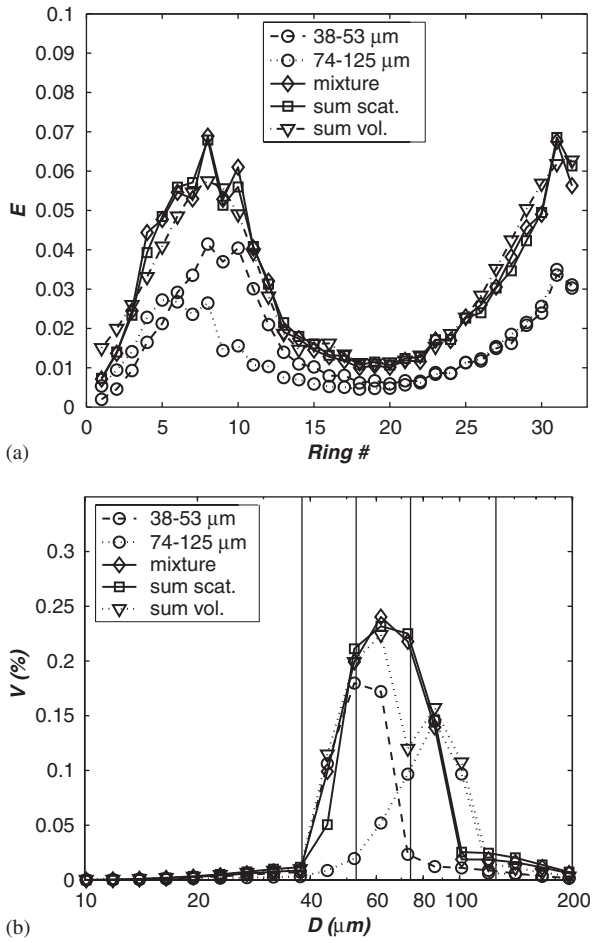

Fig. 10. Scattered light pattern (a) and inverted size distribution (b) for a bimodal suspension assumed to be composed by [55% (38–53 μm) + 45% (125–149 μm)] according to the relative concentration that gives the best combined scattering distribution, as described in Section 5.2.

distributions (Points 2, 3 and 4) appear very similar between each other.

To characterize the maximum resolution that may be achieved a test similar to the previous one was run but using two closer particles sizes, 38–53 μm and 74–125 μm. The mixing problem was present in this case too, and the results presented in Figs. 9 and 10 correspond to the raw data using the mass proportions in the original mixture and the proportions that give a best combined scattered power distribution. For this case the power signal adjustment obtained by adding the monosize distribution power signals is very good. However, the two peaks in the distribution are not correctly recovered in any case suggesting that the maximum possible resolution was achieved. Note that in this last case (38–53 μm and 74–125 μm) only one size class separates the two peaks of the size distribution obtained by adding the two monosize distributions. In the first case, two size classes were clearly separating the two peaks. Therefore, it seems that with two or more size classes in between the peaks the present algorithm is able to recover independent size classes, depending to certain extend on the relative amount of particles in each size class. The resolution obtained is on the limit of the maximum resolution possible due to the condition of the kernel matrix (Hirleman, 1987), as well as the maximum resolution obtained by the IPA algorithm (Pedocchi and García, 2006).

5.3. Settling experiments

Different settling experiments were analyzed using the 8 size class Matlab code for LISST-ST provided by Sequoia Scientific Inc. One representative result is shown in Fig. 11. It is clear from the plots that the settling history reported by the instrument does not fit the theoretical model. Therefore, the fitting of a theoretical concentration history in the form of Eq. (12) gives poor estimations of both initial concentration and settling velocity.

Evaluation of the settling velocity measurement capabilities of the LISST-ST with glass spheres were reported by Agrawal and Pottsmith (2000). The reported settling velocity estimations in such case were in fairly good agreement with Stokes settling law, although consistently higher than the predictions of Stokes'. With natural sediments, whose particles can hardly be considered spherical, different kinds of problems were reported. Researchers usually associate them with physical processes in the settling column such as flocculation of the finer fraction, convection processes in the settling column, or the presence of particles of different densities (Agrawal and Pottsmith, 2000; van Wijngaarden and Roberti, 2002).

As shown in Section 4.1, no large deviations in the concentration history can be attributed to the inversion process. Therefore, they should be attributed to problems involving the light scattering physics or deviations from the ideal particle settling law. According to the results on suspension settling velocities showed in Section 2, the fluctuations on the settling velocity tend to give broader settling fronts than the ones expected by just considering the different sizes inside a size class (Bergougnoux et al.,

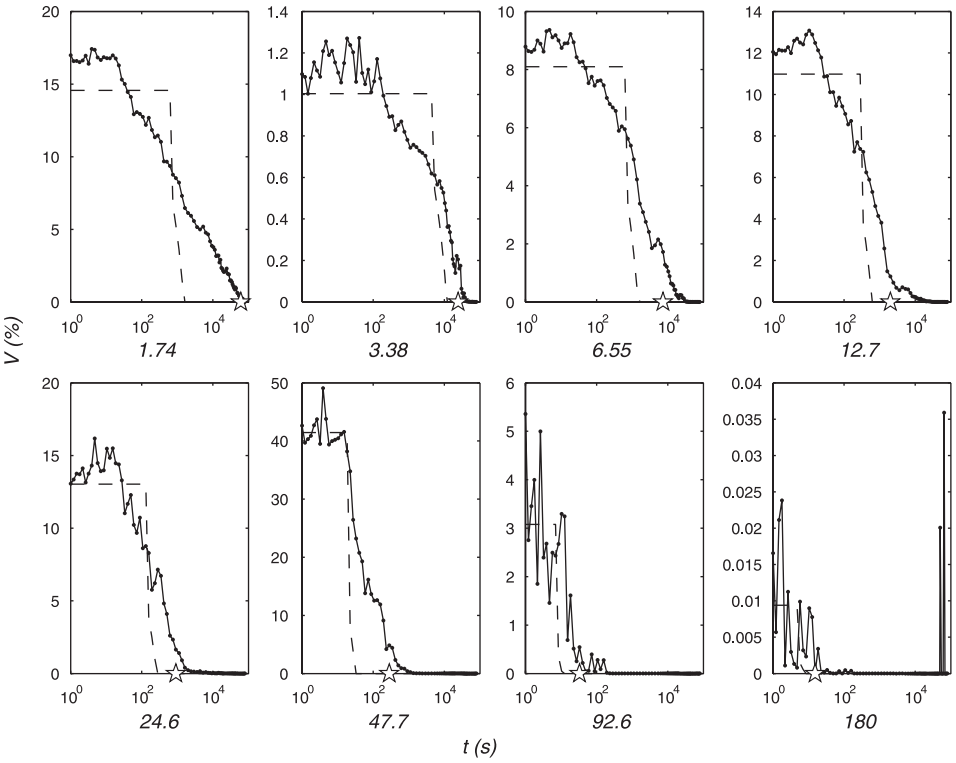

Fig. 11. Concentration histories expressed as percentage of the initial concentration for the 8 size classes solved with the Sequoia Scientific Inc. Matlab based code for the LISST-ST. The number under each plot is the mean size of the size class in μm. The solid lines are the measured concentrations, the dashed lines are the best-fit theoretical concentration histories. The starts on the time axes indicate the settling time selected by eye inspection.

2003), but this effect could only partly explain the lower slopes observed in the settling histories in Fig. 11. It is relevant to note that the summarized experiments were conducted with basically uniform particle size distributions and it is not clear what the behavior of a mixture of different sizes would be. There are some results for the possible interaction among two particles of different sizes during a settling experiment (Han and Lawler, 1991), but not for a suspension composed by many particles. In any case, the summarized effects can only have a limited influence and they can never explain the changes of an order of magnitude on the settling velocities obtained by fitting the settling model from Eq. (12) to the experiments. Also, the possible effect of the particle shapes in the settling velocity was studied (Swamee and Ojha, 1991) but it was also disregarded because the observed settling velocities are always larger than those predicted by the Stokes law, and shape effects in general tend to make settling velocities smaller, not larger (Smith and Cheung, 2003).

The IPA algorithm was also used to solve for the 32 size classes that the LISST-ST originally measures. For the size classes with lower concentration, very similar concentration histories are restored suggesting that the restored concentrations are actually strongly affected by the other more numerous sizes. The settling histories for the highest concentrated classes of the suspension in the initial distribution were the only ones that appeared to be truly independent. However, for these latter ones, the modeled and measured concentration histories do not agree either. Averaging the 32 measured size classes in groups of 4 adjacent size classes to finally report an 8 size class distribution seems to reduce the inter-size effects and improves the quality of the reported signals, but the concentration history for each of these 8 size classes is far from the theoretical model. A possible reason for this is that inter-size effects between non-adjacent size classes are not necessary negligible for irregular particles. These inter-size effects can also be observed by analyzing the measured size distribution evolution during the

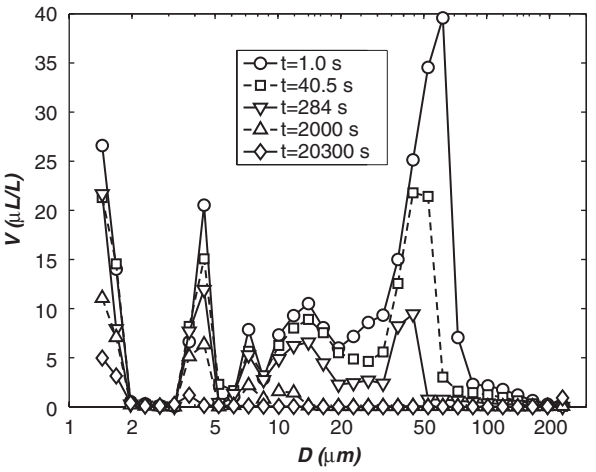

Fig. 12. Measured evolution of a size distribution of a suspension of ground silica (density 2650 kg/m^3) in the bottom of the settling column during a settling experiment in still water at 22 °C. The showed times are 1, 40.5, 284, 2000 and 20,300 s. The IPA algorithm was used to invert the power signal.

settling experiment. The size distributions for different times ($t = 1$, 40.5, 284, 2000 and 20,300 s) are shown in Fig. 12. Although only the concentration of the largest size in the suspension should decrease from one instant to the next, as in Fig. 2, in Fig. 12 the concentration of all sizes decreases over time.

Analyzing many different experiments, we found that in general the concentration histories present four different parts as time increases. First, a horizontal segment, followed by two segments with different slopes and, in many cases, a small horizontal step between these two segments. Finally, an almost horizontal portion very close to zero concentration, which clearly can be associated with noise present into the signal. This behavior can be observed in the plots showed in Fig. 11 as well as the figures presented by Agrawal and Pottsmith (2000) for glass spheres. Note that in Fig. 11 the two largest sizes do not match this description, showing concentration histories closer to the theoretical ones. In addition, as the size decreases, the deviation from the theoretical behavior becomes more and more significant, suggesting the influence of the larger sizes over the smaller ones. The interpretation of the first sloped segment in the concentration history as the product of light scattering from the larger sizes over the smaller size classes gives an alternative explanation to the results of van Wijngaarden and Roberti (2002). These authors used a non-linear fit to the concentration histories to take into account the eventual existence of two different particle densities inside each size class. They reported that especially for the smaller size classes the highest computed density was not possible to find in nature. This highest density corresponds to the first sloping section, where the influence of the larger sizes makes the concentration of the smallest sizes to decreases artificially fast.

Except from the smallest size class, the last sloped segment of the measured concentration histories present a slope very close to that given by the theoretical model. This suggests that the concentration measurements were biased by the light scattered by particles larger than the studied size class. During the recording of the last sloped segment, no particles larger than the maximum size within the class remained in suspension. Therefore, the observed variation in the concentration would correspond to the actual settling of the particles within each size class. Base on this observation, it is recommended to estimate the settling time for each size class looking for the segment of the concentration history where the slope is closer to the theoretical one and extrapolate it to the time axis. With this time value, the settling velocity for each size class can be computed using Eq. (2). The settling velocities computed by visual inspection and from the fitting of the theoretical model to the concentration histories using the software provided by Sequoia Scientific Inc. for the 8 size classes in Fig. 11 are presented in Fig. 13, showing a clear

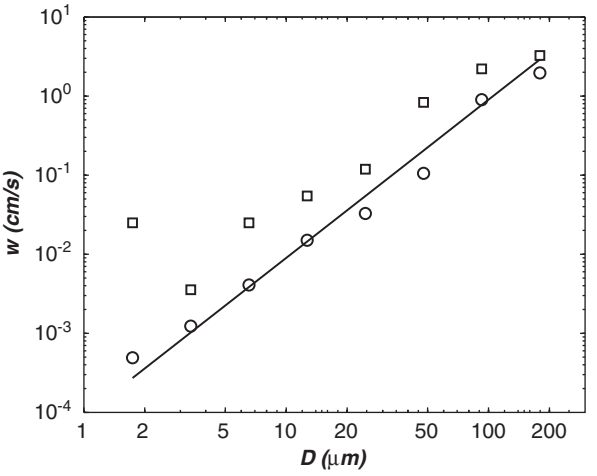

Fig. 13. Comparison of the settling velocity estimations using the two different techniques indicated in Fig. 11 for ground silica. Theoretical concentration history fitting (squares); visual estimation (circles); and Stokes' settling law for spheres (line).

improvement on the settling velocity estimations. The Stokes settling law, which can be considered an upper limit for an irregular particle settling velocity, is presented for comparison.

Finally, the lengths of the first horizontal segment in the concentration histories showed in Fig. 11 are almost the same for all sizes, suggesting that the initial size distribution is biased by non adjacent inter-size effects. On the other hand, the horizontal step between the two slope segments could be understood as period of constant concentration without the influence of the larger sizes, and therefore this concentration value might be considered as the actual concentration of the size class.

6. Conclusions and recommendations

The ability of the LISST-ST instruments to measure concentrations and size distributions was evaluated (some results may be extended to the LISST-100 instruments). This analysis focused on the main steps that are needed to get the final data: the physics of the scattering and the mathematics of the inversion algorithm.

The improved projection algorithm presented here showed to have higher resolution than the inversion algorithm that it is provided by the manufacturer of the instrument. This improves the accuracy of the concentrations and size distribution estimations of the LISST-100 which works with 32 size classes. However, this improvement is not as important for the LISST-ST which only works with 8 size classes.

The literature review suggests that the scattered light pattern of natural particles might be significantly different from that of spheres. Therefore, the size distribution obtained by inverting this natural particle light pattern using a kernel matrix that was computed for spheres could give poor estimations of the particle size distribution. The settling experiments confirm that this phenomenon is probably the main source of deviation on the settling histories. We know that Sequoia Scientific Inc. is aware of this problem and that Agrawal and colleagues are working to improve the laser scattering technique for natural particles measurements. They also found significant differences in the scattering properties of natural particles compared to those of spheres (Agrawal, personal communication), which is in agreement with the conclusions we arrived here, independently.

Regarding aggregates, it is expected that compact aggregates would behave like solid particles. However, in less compact structures the individual particles or the smaller micro-aggregates that form those structures may scatter the light as individual entities, making impossible in this case to obtain the actual size distribution of the aggregate suspension from light scattering measurements. Also, these less compact aggregates are more fragile, and they will probably break-up during the LISST-ST sampling process.

In the light of these results, the fitting of a theoretical model to the concentration history in order to compute the initial concentration and the settling velocities in the LISST-ST is not recommended. Instead, the settling velocities should be computed by analyzing the concentration histories looking for the last sloped segment of the concentration history where the slope is closer to the theoretical one and extrapolating it to the time axis to obtain the settling time for each size class. It is not clear at this time which value of the concentration history should be used to compute the initial concentration for each particle size. One possibility is to use the concentration of the first scans, though these values are probably biased by the influence of the larger particles. Another option is to use the small horizontal step, between the two sloped segments in the concentration history, as estimation of the concentration at that size class. However, further work is needed to have a final conclusion about this issue. The values of the size distribution and the settling velocities computed in the above way should be considered as a first approximation and the conclusions that the user draws from these values should take this into account.

The presented experiments showed that the mixing of the samples may be an important source of deviation in both size distribution and concentration estimates. Our experimental setup did not allow us to improve the mixing in our experiments and perform tests like the ones conducted by Gartner et al. (2001) but with the addition of simultaneous measurement of the light transmission to definitely validate the insufficient mixing hypothesis. The mixing problem may also be present in other instruments that use different measuring techniques, but with the LISST-100 and LISST-ST instruments this problem can be detected thanks to the simultaneous measurement of the area distributions and the laser transmission. Therefore, it is always important to analyze these two quantities in

order to validate the data and researchers are encouraged to report the transmission values together with the size distribution and concentration measurements.

Acknowledgments

This research was conducted under the Coastal Geosciences Program of the US Office of Naval Research as part of the EuroStrataform Project (Grants N00014-03-1-0143 and N00014-01-1-0337). F. Pedocchi was also supported by a fellowship from the Organization of American States. This support is gratefully acknowledged. The authors would like to thank Yogi Agrawal and Ole Mikkelsen for their useful suggestions during the revision of this article. Also thanks to Yovanni A. Cataño, Juan E. Martín and Blake J. Landry for their help preparing this article.

References

ASTM D422-63, 2002. Standard test method for particles-size analysis of soils. ASTM International. WWW Page, www.astm.org

Agrawal, Y.C., Pottsmith, H.C., 1994. Laser diffraction particle sizing in STRESS. Continental Shelf Research 14 (10/11), 1101–1121.

Agrawal, Y.C., Pottsmith, H.C., 2000. Instruments for particle size and settling velocity observations in sediment transport. Marine Geology 168, 89–114.

Al-Chalabi, S.A.M., Jones, A.R., 1993. Development of a Mathematical Model for Light Scattering by Statistically Irregular Particles. Particle and Particle Systems Characterization 11, 200–206.

Baker, E.T., Lavelle, J.W., 1984. The effect of particle size on the light attenuation coefficient of natural suspensions. Journal of Geophysical Research 89 (C5), 8197–8203.

Batchelor, G.K., 1972. Sedimentation in a dilute dispersion of spheres. Journal of Fluid Mechanics 52 (2), 245–268.

Bergougnoux, L., Ghicini, S., Guazzelli, E., Hinch, J., 2003. Spreading fronts and fluctuations in sedimentation. Physics of Fluids 15 (7), 1875–1887.

Chahine, M.T., 1970. Inverse problems in radiative transfer: determination of atmospheric parameters. Journal of Atmospheric Sciences 27, 960–967.

Clifford, N.J., Richards, K.S., Brown, R.A., Lane, S.N., 1995. Laboratory and Field Assessment of an Infrared Turbidity Probe and its Response to Particle Size and Variation in Suspended Sediment Concentration. Hydrological Sciences 40 (6), 771–791.

Creed, E.L., Pence, A.M., Rankin, K.L., 2001. Inter-comparison of turbidity and sediment concentration measurements from an ADP, an OBS-3, and a LISST. In: Proceeding of the Oceans 2001, MTS/IEEE, Honolulu Hi, 3, pp. 1750–1754.

de Boer, G.B.J., de Weerd, C., Thoenes, D., Goznes, H.W.J., 1987. Laser diffraction spectrometry: Fraunhofer diffraction versus Mie scattering. Particle and Particle Systems Characterization 4, 14–19.

Eisma, D., Bale, A.J., Dearnaley, M.P., Fennessy, M.J., van Leussen, W., Maldiney, M.A., Pfeiffer, A., Wells, J.T., 1996. Intercomparison of in situ suspended matter (floc) size measurements. Journal of Sea Research 36 (1/2), 3–14.

Fischbach, F.A., Brooks, S., Bond, J., 1885. Interpretation of small-angle light-scattering maxima of single-oriented microparticles. Optics Letters 10 (11), 523–525.

Fugate, D.C., Friedrichs, C.T., 2002. Determining concentration and fall velocity of estuarine particle populations using ADV, OBS and LISST. Continental Shelf Research 22, 1867–1886.

Gartner, J.W., Cheng, R.T., Wang, P., Richter, K., 2001. Laboratory and field evaluations for the LISST-100 instrument for suspended particle size determinations. Marine Geology 175, 199–219.

Gustafson, B.Å.S., 1999. Microwave analog to light scattering measurements. In: Mishchenko, M.I., Hovenier, J.W., Travis, L.D. (Eds.), Light Scattering by Nonspherical Particles: Theory, Measurements, and Geophysical Applications. Academic Press, San Diego, pp. 367–390.

Han, M., Lawler, D.F., 1991. Interactions of two settling spheres: settling rates and collision efficiency. Journal of Hydraulic Engineering, ASCE 117 (10), 1269–1289.

Hirleman, E.D., 1987. Optimal Scaling of the inverse Fraunhofer diffraction particle sizing problem: the linear system produced by quadrature. Particle and Particle Systems Characterization 4, 128–133.

Hovenier, J.W., 2000. Measuring scattering matrices of small particles at optical wavelengths. In: Mishchenko, M.I., Hovenier, J.W., Travis, L.D. (Eds.), Light Scattering by Nonspherical Particles: Theory, Measurements, and Geophysical Applications. Academic Press, San Diego, pp. 355–365.

Hovenier, J.W., Volten, H., Muñoz, O., van der Zande, W.J., Waters, L.B.F.M., 2003. Laboratory studies of scattering matrices for randomly oriented particles: potentials, problems, and perspectives. Journal of Quantitative Spectroscopy & Radiative Transfer 79–80, 741–755.

Huang, T.S., Barker, D.A., Berger, S.P., 1975. Iterative Image Restoration. Applied Optics 14 (5), 1165–1168.

Jianping, W., Shizhong, X., Yimo, Z., Wei, L., 2001. Improved projection algorithm to invert forward scattered light for particle sizing. Applied Optics 40 (23), 3937–3945.

Jones, A.R., 1987. Fraunhofer diffraction by random irregular particles. Particle Characterization 4, 123–127.

Liu, L., Mishchenko, M.I., Hovenier, J.W., Volten, H., Muñoz, O., 2003. Scattering matrix of quartz aerosols: comparison and synthesis of laboratory and Lorenz–Mie results. Journal of Quantitative Spectroscopy & Radiative Transfer, 79–80, 911–920.

Lynch, J.F., Irish, J.D., Sherwood, C.R., Agrawal, Y.C., 1994. Determining suspended sediment particle size information from acoustical and optical backscatter measurements. Continental Shelf Research 14 (10/11), 1139–1165.

Manning, A.J., Dyer, K.R., 1999. A laboratory examination of flock characteristics with regard to turbulent shearing. Marine Geology 160, 147–170.

Matsuyama, T., Yamamoto, H., Scarlett, B., 2000. Transformation of diffraction pattern due to ellipsoids into equivalent diameter distribution for spheres. Particle and Particle Systems Characterization 17, 41–46.

McCave, I.N., Gross, T.F., 1991. In-situ measurements of particle settling velocity in the deep sea. Marine Geology 99, 403–411.

Mikkelsen, O.A., Milligan, T.G., Hill, P.S., Moffatt, D., 2004. INSSECT—an instrumented platform for investigating floc properties close to the seabed. Limnology & Oceanography: Methods 2, 226–236.

Mikkelsen, O.A., Hill, P.S., Milligan, T.G., Chant, R.J., 2005. In situ particle size distributions ans volume concentrations from a LISST-100 laser particle sizer and a digital flock camera. Continental Shelf Research 25, 1959–1978.

Mühlenweg, H., Hirleman, E.D., 1998. Laser diffraction spectroscopy: influence of particle shape and shape adaptation technique. Particle and Particle Systems Characterization 15, 163–169.

Mühlenweg, H., Hirleman, E.D., 1999. Reticles as Standards in Laser Diffraction Spectroscopy. Particle and Particle Systems Characterization 16, 47–53.

Muñoz, O., Volten, H., de Haan, J.F., Vassen, W., Hovenier, J.W., 2001. Experimental determination of scattering matrices of randomly oriented fly ash and clay particles at 442 and 633 nm. Journal of Geophysical Research 106 (D19), 22833–22844.

Pedocchi, F., García., M.H., 2006. Noise-Resolution trade-off in Projection Algorithms for Laser Diffraction Particle Sizing. Applied Optics 45 (15).

Riley, J.B., Agrawal, Y.C., 1991. Sampling and inversion of data in diffraction particle sizing. Applied Optics 30 (33), 4800–4817.

Segrè, P.N., Herbolzheimer, E., Chaikin, P.M., 1997. Long-range correlations in sedimentation. Physical Review Letters 79 (13), 2574–2577.

Sequoia Scientific Inc., 2005. Frequently Asked Questions, LISST. WWW Page, http://www.sequoiasci.com/faq/faq-question.aspx?faqquestion=43

Smith, D.A., Cheung, K.F., 2003. Settling characteristics of calcareous sand. Journal of Hydraulic Engineering, ASCE 129 (6), 479–483.

Stone, S., Bushell, G., Amal, R., Ma, Z., Merkus, H.G., Scarlett, B., 2002. Characterization of large fractal aggregates by small-angle light scattering. Measurement Science and Technology 13, 357–364.

Swamee, P.K., Ojha, C.S.P., 1991. Drag coefficient and fall velocity of nonspherical particles. Journal of Hydraulic Engineering, ASCE 117 (5), 660–667.

Twomey, S., 1977. An Introduction to the Mathematics of Inversion in Remote Sensing and Indirect Measurements. Elsevier, Amsterdam.

Traykovski, P., Latter, R.J., Irish, J.D., 1999. A laboratory evaluation of the laser in situ scattering and transmissometery instrument using natural sediments. Marine Geology 159, 355–367.

van de Hulst, H.C., 1981. Light Scattering by Small Particles. Dover Publications, Inc., New York.

van Wijngaarden, M., Roberti, J.R., 2002. In situ measurements of settling velocity and particle distribution with the LISST-ST. In: Winterwerp, J.C., Kranenburg, C. (Eds.), Fine Sediment Dynamics in the Marine Environment. Elseiver Science B.V., Amsterdam, pp. 295–311.

Volten, H., Muñoz, O., Rol, E., de Haan, J.F., Vassen, W., Hovenier, J.W., Muinonen, K., Nousiainen, T., 2001. Scattering matrices of mineral particles at 441.6 nm and 632.8 nm. Journal of Geophysical Research 106 (D15), 17375–17401.

Volten, H., de Haan, J.F., Hovenier, J.W., Schreurs, R., Vassen, W., Dekker, A.G., Hoogenboom, H.J., Charlton, F., Wouts, R., 1998. Laboratory measurements of angular distributions of light scattered by phytoplankton and silt. Limnology and Oceanography 43, 1180–1197.

Wedd, M.W., 2003. Determination of particle size distributions using laser diffraction. Educational Resources for Particle Technology, 032Q-Weed, WWW Page, http://www.erpt.org/032Q/Wedd-00.htm

Wren, D.G., Barkdoll, B.D., Kuhnle, R.A., Derrow, R.W., 2000. Field techniques for suspended-sediment Measurement. Journal of Hydraulic Engineering, ASCE 126 (2), 97–104.